University of Thi-Qar Journal of Science (UTJsci)
E-ISSN: 2709-0256, P-ISSN: 1991-8690, Vol. 12, No. 2, Dec. 2025

DFT Study of Cu_2O/Carbon-Based Nanomaterials Interacting with Zn and ZnS

Ahmed Ibrahim[1 a*] , Abbas Shwya[2b], Soukaina B.[3c] and Pr. Larbi Setti[4d]

[1,2] *Department of Physics, Faculty of Science, University of Thi-Qar, Nasiriyah, Iraq.*
[3,4] *Abdelmalek Essaadi University, Larache, Morocco, Tetouan, Morocco*

[b]E-mail: abbas.alwan@sci.utq.edu.iq , [c]E-mail:soukaina.bouhmaidi@etu.uae.ac.ma, [d]E-mail: lsetti@uae.ac.ma
[a*]Corresponding author: ahmed_ibra.phy@utq.edu.iq

Received: 2025-07-30, Revised: 2025-09-18, Accepted: 2025-10-18, Published: 2025-12-12

Abstract*—Copper oxide (I)/carbon-based nanomaterials have a great attention nowadays due to their potential in electronic and thermoelectric applications. In this study, density functional theory (DFT) was applied using the B3LYP hybrid function and the B3LYP 6-31G basis set to study the properties of ($6Cu_2O/C_{17}$) and ($4Cu_2O/C_8$) structures, as well as their interactions with zinc sulphide (ZnS) and zinc (Zn). The calculations included the determination of molecular geometry, contour density maps, electrostatic potential surfaces, spectra, HOMO and LUMO energies, band gap, dipole moment, polarizability, point group symmetry, and three states (DOS). The results showed that the interaction between ($6Cu_2O/C_{17}$) and (Zn, ZnS) led to a clear charge transfer and exchange, which was reflected in the density and electrostatic potential maps. The structures ($6Cu_2O/C_{17}$), ($6Cu_2O/C_{17}$–Zn), and ($6Cu_2O/C_{17}$–ZnS) also revealed narrow band gaps (~0.3 eV), which enhances their thermoelectric properties. Furthermore, interaction with ZnS increased the dipole moment from (2.99 Debye) to (15.33 Debye), indicating its potential for use in high dielectric materials. The ($4Cu_2O/C_8$) structure showed Cs group symmetry, which makes it important for optical applications. DOS maps also showed the emergence of new energy states resulting from interaction with Zn and ZnS. These results demonstrate that the studied nanostructures possess promising electronic, optical, and thermoelectric properties, qualifying them for practical applications in energy conversion and advanced device fabrication.

Keywords—DFT, Symmetry, Dipole moment, Copper (I) oxide, Zinc sulfide

I. INTRODUCTION

The electronic structure of particular atoms, molecules, nanoclusters, and substances can be studied using quantum mechanical techniques such as density functional theory, post Hartree-Fock methods, and the Hartree-Fock approximation [1]. Density functional theory (DFT) is employed for studying systems with many particles throughout the electron density [2]. Electron density is the probability of finding electrons at a given point in space [3]. According to density functional theory, the electron density is more significant than the wave function and solely depends on three spatial dimensions, independent of the electrons' location within the system. By comparison, the wave function approximation considers three parameters: three spatial coordinates, one spin coordinate, and the fixed nuclei position assumption [4]. Using this theory, the properties of a multi-electron system can be ascertained by studying the functionals, which stand for functions of another functions [5]. In computational physics and chemistry, DFT is one of the most popular methods for figuring out the electronic properties of solid state materials [6]. The outcomes of DFT calculations substantially resemble the experimental results when applied to solid state systems [7]. Hohenberg-Kohn proposed density functional theory in two research publications in the 1960s [8]. DFT was not thought to be accurate enough for calculations involving quantum chemistry until the 1990s [9]. By disregarding the system's wave function, DFT seeks to determine the ground state energy of N electron system solely from its density [10]. DFT is computationally developed by John Pople using notions from quantum chemistry. Pople and Walter Kohn were awarded the 1998 Nopel Prize in Chemistry because they contributed to enhance the calculations of DFT [11]. The material utilized in this paper were Zinc (Zn), Zinc Sulfide (ZnS), $4Cu_2O/C_8$ and $6Cu_2O/C_{17}$. One nanomaterial that was utilized in the manufacture of semiconductors is zinc sulfide. The organic complexes that based on mixing Cu_2O and carbon are employing in numerous scientific fields [12]. Cu_2O (p-type) systems with Zn or ZnS (n-type) form p–n interfaces that improve charge separation and reduce recombination, thereby enhancing electronic and optical performance. The wide bandgap of ZnS, when combined with Cu_2O, allows for effective band alignment that facilitates electron transport and enhances catalytic and electrochemical properties. Zn doping/insertion also

https://doi.org/10.32792/utq/utjsci/v12i2.1457

adjusts the band gap and conductivity, while the incorporation of Cu_2O with carbon enhances charge transport and electronic stability [13-16]. The goal of study is to find out organic complex nanomaterial structures during the interactions between the organic complexes that based on copper (I) oxide (Cu_2O) and carbon and it's interactions with zinc and zinc sulfide, in order to enhance the electronic characteristics, optical merits and thermoelectric properties. The study aims was to improve the organic complexes nanomaterial structures to become more appropriate for electronic devices, just like, transistors, diodes and integrating circuits and thermoelectric devices, such as energy conversion devices which convert the heat energy into the electric energy.

A. *Computational Details*

All theoretical calculations were performed using Gaussian 09 [17] based on density functional theory (DFT), which is one of the most accurate and efficient ways to describe the electronic and physical properties of compounds. The B3LYP hybrid function was chosen due to its high accuracy in representing the behavior of organic and inorganic molecules [18], while the 6-31G basis set was used for all atoms under study [19]. The calculations were carried out using the Frequency Analysis option, through which the IR spectra were obtained and the stability of the optimized structures was verified by the absence of any imaginary frequency values. Additional properties such as dipole moment and polarizability were extracted. In addition, HOMO and LUMO levels were calculated and the energy gap in electron-volt (eV) were deduced to evaluate the electronic activity of the compounds. The density of electronic states (DOS) was analyzed using Gaussian-related Gauss View software, enabling a deeper understanding of the energy distribution of molecular orbitals.

Nanostructure	Mode No.	Frequency (cm^{-1})	IR Intensity (a.u.)	Assignment
($6Cu_2O/C_{17}$–Zn)	1	495	40	Cu–O–Zn stretching
	2	742	35	C–C vibration
	3	1158	58	C–O stretching
	4	1605	71	C=C stretching
	5	2992	83	C–H stretching (aliphatic)
	6	3110	91	C–H stretching (aromatic)
($6Cu_2O/C_{17}$–ZnS)	1	488	47	Cu–O–S stretching
	2	690	30	Zn–S vibration
	3	1132	64	C–O stretching
	4	1582	79	C=C stretching
	5	2978	86	C–H stretching (aliphatic)
	6	3105	93	C–H stretching (aromatic)

The symmetry elements of the studied structures were determined based on the results of the frequency analysis, in order to deduce the symmetric properties of the compounds.

II. Results and Discussion

A. *Molecular Geometry*

Molecular structure is expressed by the positions of the atoms within the structure or the system. The molecular geometry of many bodies structures depends on several factors, as well, the repulsion forces among the electrons, electrons penetrations towards the nuclei and the shielding of the electrons by the nuclei [20]. The molecular geometry of the nanomaterial structures $4Cu_2O/C_8$, $6Cu_2O/C_{17}$, ($4Cu_2O/C_8$)-Zn, ($4Cu_2O/C_8$)-ZnS, ($6Cu_2O/C_{17}$)-Zn and ($6Cu_2O/C_{17}$)-ZnS were carried out by employing density functional theory at the ground state energy and the basis set 6-31G with hybrid functional B3LYP.

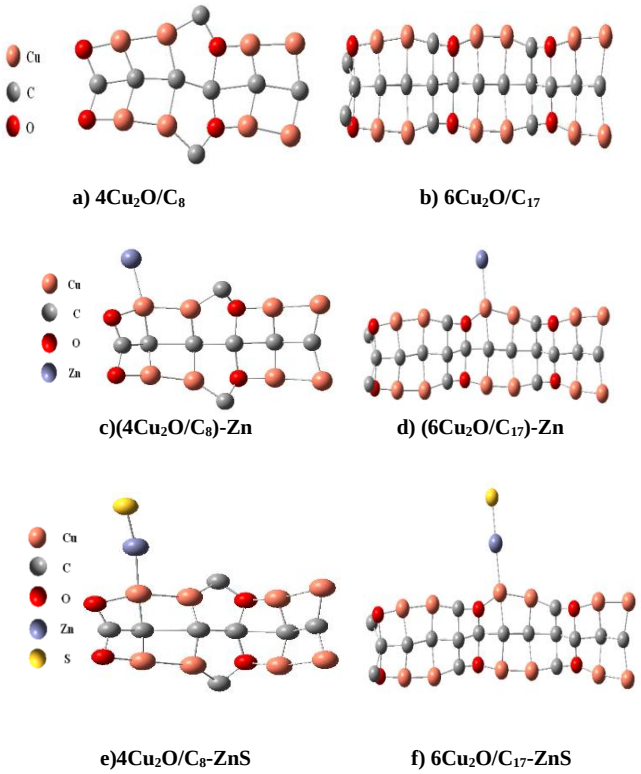

Figure (1): The molecular geometry of the nanomaterial structures $4Cu_2O/C_8$, $6Cu_2O/C_{17}$, ($4Cu_2O/C_8$)-Zn, ($4Cu_2O/C_8$)-ZnS, ($6Cu_2O/C_{17}$)-Zn and ($6Cu_2O/C_{17}$)-ZnS.

Figure (1) demonstrates the copper atoms with orange color, oxygen atoms with red color, the carbon atoms with lead color, zinc atoms with light blue color and sulfur atoms with yellow color. Copper (I) oxide (Cu_2O) is classified as a semiconductor, and it has tendency to make a covalent bond. Each carbon atom owns four electrons in the outer shell, therefore carbon atoms have the tendency to make a covalent bonds. Zinc (Zn) is classified as a metal, therefore, it has the tendency to donate the electrons from the outer shell. Hence, when zinc atom interacts with the complex nanostructure ($4Cu_2O/C_8$) or the complex nanostructure ($6Cu_2O/C_{17}$), the result bonds will not be pure covalent and will not be

pure ionic bond. The bond may be partially covalent and ionic. Physical phenomena may be occur near the surface at the interaction region between the surfaces of the nanomaterial structures ($4Cu_2O/C_8$, $6Cu_2O/C_{17}$) and zinc (Zn) atom. The physical phenomena include adsorption, physisorption, charge exchange or charge transfer. The absence of imaginary frequencies (negative values) after optimizing the structure indicates that the structure located at a real minimum point on the potential energy surface, while having a suitable (non-zero) energy band gap (LUMO_HOMO) indicates an electronic stability. Having a large\ band gap means a higher resistance to random electronic transitions. Znic sulfide (ZnS) is classified as a wide band gap semiconductor, when zinc sulfide interacts with ($4Cu_2O/C_8$) or ($6Cu_2O/C_{17}$) tend to consistence of hetro-junction, like this interaction is considered very interested in the photocatalytic and electrochemical properties.

B. Electrostatic Potentials

HOMO and LUMO surfaces have been visualized by updating the molecular structure through the choice MOs, in which MOs means molecular orbital theory. In this theory, the atomic orbitals merged to consistence molecular orbitals. They are the frontier orbitals in which they determine the energy band gap merit, which is utilized to determine types of the materials (conductor, semiconductor or insulator). The difference between LUMO energy and HOMO energy yields the energy gap [21]. Density functional theory method had been utilized to carry out the electrostatic potential for $4Cu_2O/C_8$, $6Cu_2O/C_{17}$, ($4Cu_2O/C_8$)-Zn, ($4Cu_2O/C_8$)-ZnS, ($6Cu_2O/C_{17}$)-Zn and ($6Cu_2O/C_{17}$)-ZnS at the ground state energy and the basis set 6-31G with hybrid functional B3LYP.

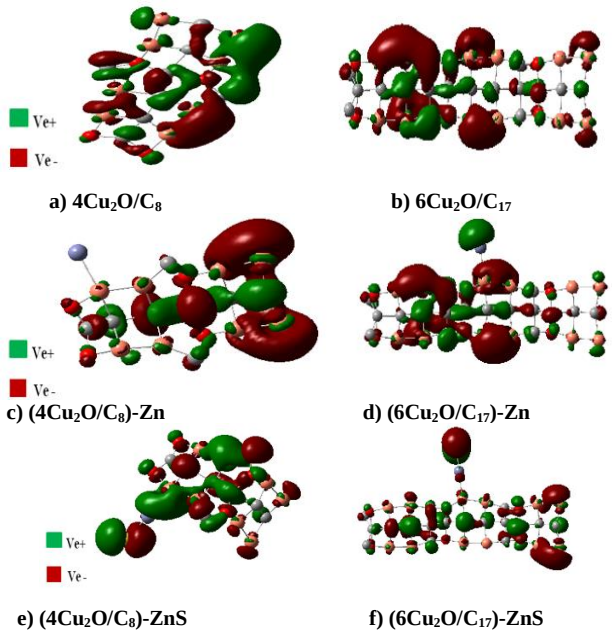

Figure (2): The electrostatic potentials of the nanomaterial structures $4Cu_2O/C_8$, $6Cu_2O/C_{17}$, ($4Cu_2O/C_8$)-Zn, ($4Cu_2O/C_8$)-ZnS, ($6Cu_2O/C_{17}$)-Zn and ($6Cu_2O/C_{17}$)-ZnS.

Figure (2) demonstrates dissimilarity in the charge distribution about the atoms when the zinc atom interacts with the nanomaterial structure $6Cu_2O/C_{17}$. The interaction between zinc atom and $6Cu_2O/C_{17}$ leads to a charge distribution around the zinc atom, and causes a charge exchange in other regions in the molecular structure. This is apparent by making a simplified comparison between pictures of $6Cu_2O/C_{17}$ and ($6Cu_2O/C_{17}$)-Zn. The interaction between the nanomaterial structure $4Cu_2O/C_8$ and zinc sulfide (ZnS) tends to originate the electronic charge distribution in the interaction region between $4Cu_2O/C_8$ and zinc sulfide (ZnS). The interaction depicts electronic charge distribution around zinc sulfide (ZnS) atoms. The interpretation here, if the charge exchange occurs, the nanomaterial structure $4Cu_2O/C_8$ may set a positive test charge from the nuclei of Cu_2O atoms or carbon atoms towards the surface in order to attract the electrons from the zinc sulfide. Also one can say zinc sulfide (ZnS) may set a positive test charge towards the surface to attract the electrons from the nanomaterial structure $4Cu_2O/C_8$. The green color in the electrostatic potential surface indicates to the positive partition of the wave function, but the maroon color points out the negative ve partition of the wave function. Also, when we make a comparison between $6Cu_2O/C_{17}$ and ($6Cu_2O/C_{17}$)-Zn, $4Cu_2O/C_8$ and ($4Cu_2O/C_8$)-ZnS can visualize impact of the interaction on the shape of electrostatic potential surface which denotes to the difference in the charge distribution apparently before and after the interactions.

C. Contours

Electron density contours are also represented on the electrostatic potential surfaces. It stands for a n advantageous tool to describe Fermi level. Fermi energy and Brillion zones are well known in solid state physics. In the contour maps, the active regions in the molecular structure or molecular system apparently demonstrate. The charge distribution of the electrons around the nuclei of atoms in the molecular system depicts in the density contour maps. Therefore occasionally contour maps are utilized to describe the charge transfer and charge exchange [22]. The contour density maps were performed using the density functional theory at the ground state, B3LYP level and 6-31G basis set for the nanomaterial structures $4Cu_2O/C_8$, $6Cu_2O/C_{17}$, ($4Cu_2O/C_8$)-Zn, ($4Cu_2O/C_8$)-ZnS, ($6Cu_2O/C_{17}$)-Zn and ($6Cu_2O/C_{17}$)-ZnS.

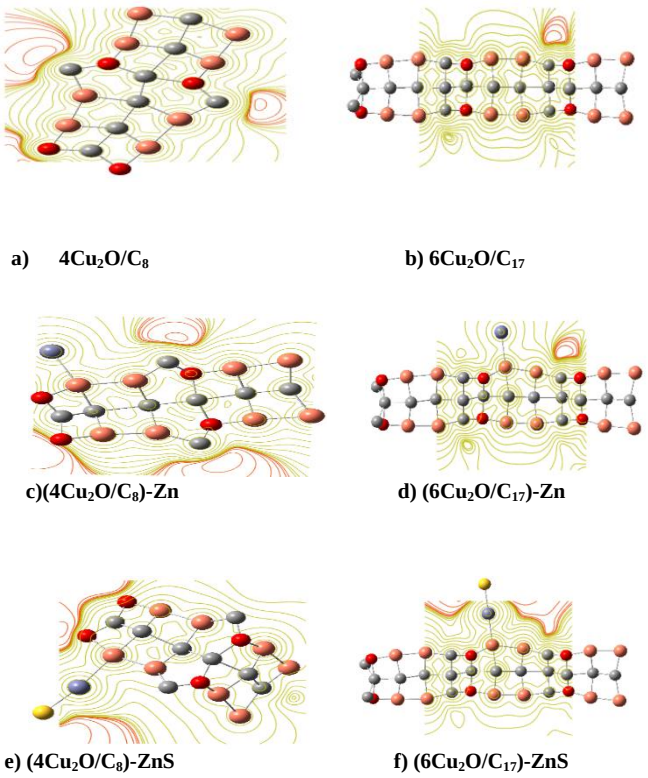

Figure (3): Contour density maps of the nanomaterial structures $4Cu_2O/C_8$, $6Cu_2O/C_{17}$, $(4Cu_2O/C_8)$-Zn, $(4Cu_2O/C_8)$-ZnS, $(6Cu_2O/C_{17})$-Zn and $(6Cu_2O/C_{17})$-ZnS.

Figure (3) demonstrates the active regions through the distortion in the contour density maps. By holding a modest comparison between $4Cu_2O/C_8$ and $(4Cu_2O/C_8)$-Zn, it can be visualized that dissimilarity in the contour maps shapes, this occurs due to the interaction between zinc atom and the atoms of the nanomaterial structure $4Cu_2O/C_8$. The charge density distribution was around the zinc atom be systematically, the active regions showed apparently around the atoms carbon and oxygen. The interpretation here, the electrons owned a tendency to stay near carbon and oxygen atoms more than the other atoms in the complex nanomaterial structure, and this happened because the electrons in the complex nanomaterial structure $(4Cu_2O/C_8)$-Zn influenced by the attraction force of the nuclei of carbon and oxygen more than zinc and copper nuclei. The electrons prefer to stay near the nuclei of carbon rather than oxygen . The atomic number of carbons is 6 and oxygen is 8, but for copper is 29 and zinc is 30. One can censor two active regions near carbon atoms, but one active a region near oxygen atoms, this takes place because the atomic number of carbon smaller than the atomic number of oxygen. The complex nanomaterial structure $(4Cu_2O/C_8)$-ZnS possesses a new site for distortion signs active region in the interaction region between zinc sulfide (ZnS) and $(4Cu_2O/C_8)$. A simple counter-posing between $6Cu_2O/C_{17}$ and $(6Cu_2O/C_{17})$-ZnS clarified existence new distortions in the contour maps right and left ZnS in the interaction region near the atoms of carbon, oxygen, sulfur and zinc. Hence, one can say that the interaction in this complex nanomaterial structure will be stronger, and the charge exchange or charge exchange will be more apparently as compared with other complexes nanomaterial structures.

D. Infrared Spectra (IR)

The infrared spectroscopy express on the interactions between the infrared spectrum and the substances. It employs to test the substances during appearance the active groups (the bonds between two atoms). Infrared spectra yield the vibration modes which can be symmetric or asymmetric. The symmetric vibration happens between atoms of the same kind, but the asymmetric vibration takes place between atoms of dissimilar kinds [23,24]. The modes might be elastic or inelastic. The infrared spectra for the nanomaterial structures $4Cu_2O/C_8$, $6Cu_2O/C_{17}$, $(4Cu_2O/C_8)$-Zn, $(4Cu_2O/C_8)$-ZnS, $(6Cu_2O/C_{17})$-Zn and $(6Cu_2O/C_{17})$-Zn had been carried out at the ground state, B3LYP level, and 6-31G basis set.

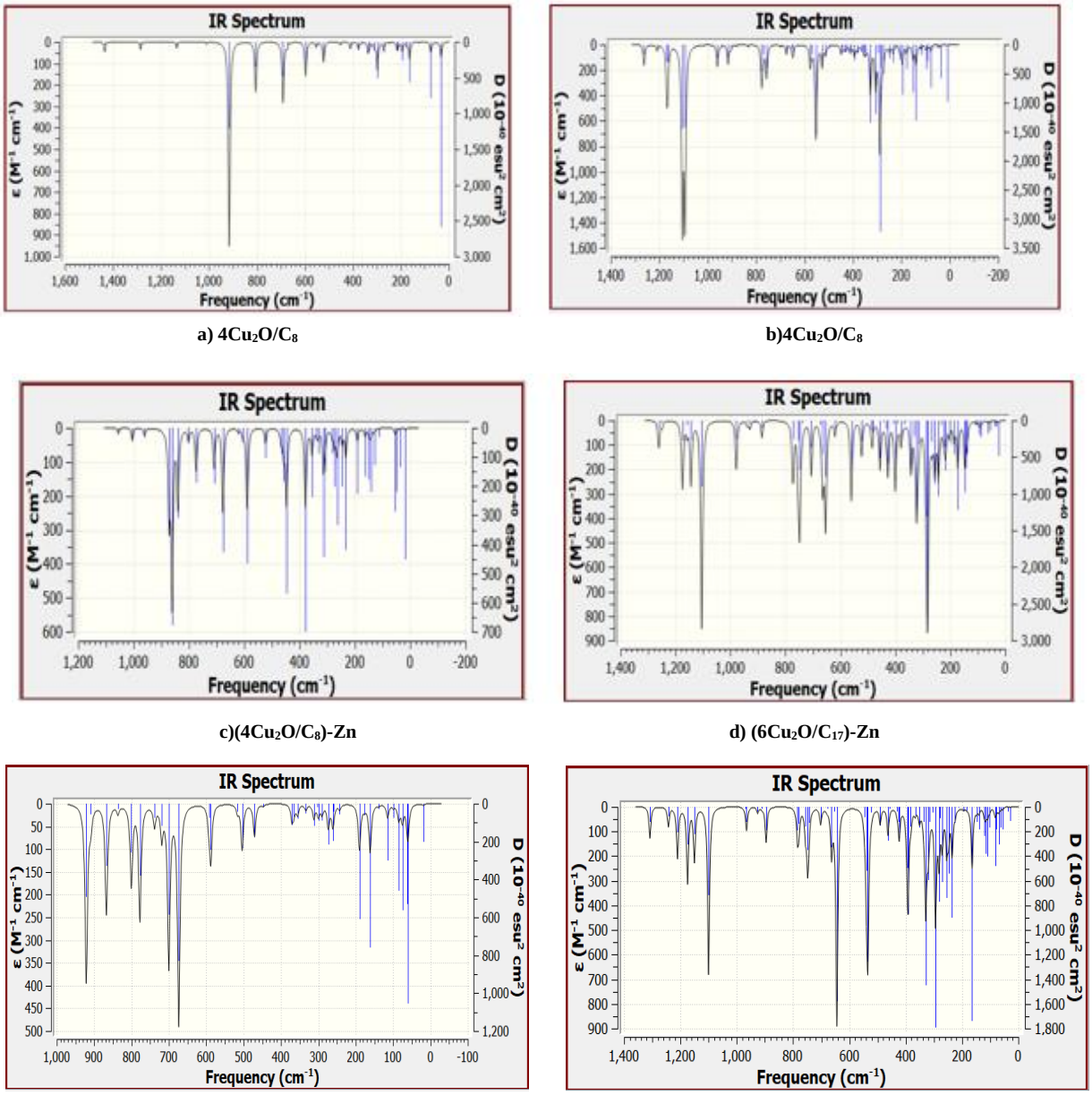

a) $4Cu_2O/C_8$ **b)$4Cu_2O/C_8$**

c)($4Cu_2O/C_8$)-Zn **d) ($6Cu_2O/C_{17}$)-Zn**

e)($4Cu_2O/C_8$)-ZnS **f)($6Cu_2O/C_{17}$)-ZnS**

Fig 4: Infrared spectra (IR) for the nanomaterial structures $4Cu_2O/C_8$, $6Cu_2O/C_{17}$, ($4Cu_2O/C_8$)-Zn, ($4Cu_2O/C_8$)-ZnS, ($6Cu_2O/C_{17}$)-Zn and ($6Cu_2O/C_{17}$)-ZnS

Table (1): illustrates HOMO, LUMO electronic states and the energy band gaps (E_g) for the nanomaterial structures $4Cu_2O/C_8$, $6Cu_2O/C_{17}$, ($4Cu_2O/C_8$)-Zn, ($4Cu_2O/C_8$)-ZnS, ($6Cu_2O/C_{17}$)-Zn and ($6Cu_2O/C_{17}$)-ZnS.

.

System	E_{LUMO} (eV)	E_{HOMO} (eV)	Energy gap (eV)
$4Cu_2O/C_8$	-4.388	-5.157	0.768
($4Cu_2O/C_8$)-Zn	-3.972	-4.933	0.960
($4Cu_2O/C_8$)-ZnS	-4.882	-5.401	0.519
$6Cu_2O/C_{17}$	-4.035	-4.357	0.322
($6Cu_2O/C_{17}$)-Zn	-3.929	-4.266	0.336
($6Cu_2O/C_{17}$)-ZnS	-4.550	-4.894	0.344

In Figure (4) when one makes a modest comparison between $4Cu_2O/C_8$ and $(4Cu_2O/C_8)$-ZnS can visualize new peaks emerge in the complex nanomaterial structure $(4Cu_2O/C_8)$-ZnS. These peaks indicated new bonds generated between (zinc , sulfur) and the atoms of the nanomaterial structure $4Cu_2O/C_8$. The peaks may be (Zn-Cu), (Zn-O), (Zn-C), (S-C), S-Cu) or (S-O). One can visualize in the nanomaterial structure $4Cu_2O/C_8$, the apex next 900 cm^{-1} be under the intensity (950 $Mole^{-1}$ cm^{-1}), but after the interaction with zinc atom, i.e. in the complex nanomaterial structure $(4Cu_2O/C_8)$-Zn, the apex next (900 cm^{-1}) became under the intensity (550 $Mole^{-1}$ cm^{-1}). The reduction in the intensity was due to a weak bond originated by means of adding the zinc impurity to the nanomaterial structure $4Cu_2O/C_8$, Zinc atoms tend to form weak covalent bonds, donating an electron pair from their valence shell to form a bond with carbon (C) or copper (Cu) atoms. As well a simplified comparison between $6Cu_2O/C_{17}$ and $(6Cu_2O/C_{17})$-Zn demonstrates the impact of zinc atom. At the wave number next (1100 cm^{-1}), the intensity was more than (1500 $Mole^{-1}$ cm^{-1}), but after the interaction with zinc atom at the same wave number, the intensity became shortly (850 $Mole^{-1}$ cm^{-1}). The interaction of zinc sulphide (ZnS) atoms with the $6Cu_2O/C_{17}$ nanostructure led to the appearance of new peaks in the spectrum. These peaks appeared at different values in terms of intensity and wave number.

E. Electronic states and energy gap (E_g)

Generally the energy band gap (E_g) stands for the energy difference between valence band and conduction band. According to density functional theory, the energy band gap typified the energy difference between the frontier orbitals LUMO and HOMO. The energy band gap is one of the most interest quantities in the solid-state physics because it determines what if the substance insulator, semiconductor or conductor [25,26]. Mathematically the energy band gap can be expressed by the following equation [27]

$$E_g = E_{LUMO} - E_{HOMO} \quad \ldots \quad (1)$$

Table 1. Shows behavior of all nanomaterial structures as a semiconductors because they have values of energy gap in the domain of semiconductor materials. The nanomaterial structures $6Cu_2O/C_{17}$, $(6Cu_2O/C_{17})$-Zn and $(6Cu_2O/C_{17})$-ZnS possess a narrow semiconductor energy gaps, they are approximately (0.32 eV), (0.33 eV) and (0.34 eV) respectively. The energy gaps of those nanomaterial structures are all near the value of energy gap (E_g) of lead telluride (PbTe). (E_g) of lead telluride is shortly 0.3 eV. This makes them as semiconductor nanomaterial structures which have an excellent performance at the medium temperature. The semiconductors with energy gap near (0.3 eV) are very advantageous in the applications conversion the heat to electric energy due to their thermoelectric characteristics. The other nanomaterial structures in the table were $4Cu_2O/C_8$, $6Cu_2O/C_{17}$, $(4Cu_2O/C_8)$-Zn. These materials have energy gaps acquire importance in many electronic devices such as transistors, diodes and integrated circuits. The HOMO energy describes the nanostructure to donate the electrons, therefore, the nanomaterial structure $(6Cu_2O/C_{17})$-Zn has greater ability for donation the electrons as compared with the nanomaterial structures in the table, because it has the maximum value of HOMO energy of (-4.26 eV). The LUMO energy expresses the nanostructure ability to accept electrons in acceptor level, therefore, the nanomaterial structure $(4Cu_2O/C_8)$-ZnS was regarded the best acceptor in the table, due to their minimum value of LUMO energy of (-5.4 eV).

F. Dipole moment and polarizabilities

The dipole moment is the result of multiplying the charge by the displacement. The direction of the displacement affects the dipole moment. The displacement between two charges, one of which is (+ve) and the other is (-ve), was represented by symbol. If the charge is represented by the symbol q, then the dipole moment (μ) equation can be expressed as follows [28]

$$\mu = q * r \quad \ldots \quad (2)$$

The property of a molecule to become polarized is referred to as "polarizability". The linear response of electron density in the presence of a seminal electric field F is another way to convey the idea of polarizability. Mathematically the polarizability can be expressed as a second-order variation of the energy [29]

$$\alpha = -\left(\frac{\partial^2 E}{\partial F_a \partial F_b}\right)_{a,b} = x, y, z \quad \ldots \quad (3)$$

Table (2): exhibits the dipole moment and average polarizability for the nanomaterial structures $4Cu_2O/C_8$, $6Cu_2O/C_{17}$, $(4Cu_2O/C_8)$-Zn, $(4Cu_2O/C_8)$-ZnS, $(6Cu_2O/C_{17})$-Zn and $(6Cu_2O/C_{17})$-ZnS.

System	μ (Debye)	Average Polarizability (a.u)
$4Cu_2O/C_8$	8.024	520.804
$(4Cu_2O/C_8)$-Zn	9.018	576.305
$(4Cu_2O/C_8)$-ZnS	15.343	645.861
$6Cu_2O/C_{17}$	2.998	1515.438
$(6Cu_2O/C_{17})$-Zn	4.898	1541.381
$(6Cu_2O/C_{17})$-ZnS	15.334	1566.183

Table (2) shows that the nanomaterial structures have no zero dipole moment, because they were all hetro-nuclear structures. The zero dipole moment only appears in the homo-nuclear structure. It was apparent that the interaction of zinc sulfide with the nanomaterial structures ($4Cu_2O/C_8$, $6Cu_2O/C_{17}$) lead to clear increasing in the value of dipole moment, i.e. each one of the complex organic nanomaterial structures $(4Cu_2O/C_8)$-ZnS and $(6Cu_2O/C_{17})$-ZnS became possesses dipole moment value more than (15.3 Debye). It is a crucial quantity for recognizing the polar and non-polar bonds. All nanomaterial structures which possess dipole moment is considered polar molecules. Knowing the values of dipole moment is regarded very beneficial for designing the optics devices. The organic complex nanomaterial

structure ($6Cu_2O/C_{17}$)-ZnS is regarded the highest activity nanomaterial structure, by means of, it has the maximum value of the average polarizability, it is about (1566.12 a.u). The polarizability has a maximum benefit in the applications of linear and nonlinear optics. One of the most important characteristics which depend on the polarizability is the optical basicity. Furthermore, the polarizability provides an information about the interatomic structure of the substances. One can visualize the average polarizability influences more by the number of atoms. The average polarizability increase as the number of atoms increases. So the dipole moment influences by the number of atoms in the organic complex nanomaterial structure, and the dipole moment increases as the number of atoms increases.

G. Symmetry

The symmetry of molecules or systems lay a vital role in the bonding because only the orbits which possess the same symmetry possess a capability to overlap or mix. For each molecular system there is a point group, there are several symmetry processes link to this point group. The special kind of symmetry which links to the symmetry of the molecules is named the symmetry element. There are symmetry operation categories for each symmetry element. The seven symmetry elements are identity, vertical plane, dihedral plane, improper axis, horizontal axis center of symmetry or inversion center and proper axis [30-32]. Density functional theory at the ground state, B3LYP level, and 6-31G basis set, had been carried out to find out the point group symmetries for the nanomaterial structures $4Cu_2O/C_8$, $6Cu_2O/C_{17}$, ($4Cu_2O/C_8$)-Zn, ($4Cu_2O/C_8$)-ZnS, ($6Cu_2O/C_{17}$)-Zn and ($6Cu_2O/C_{17}$)-ZnS.

Table (3) shows point group symmetries for the nanomaterial structures $4Cu_2O/C_8$, $6Cu_2O/C_{17}$, ($4Cu_2O/C_8$)-Zn, ($4Cu_2O/C_8$)-ZnS, ($6Cu_2O/C_{17}$)-Zn and ($6Cu_2O/C_{17}$)-ZnS.

System	Symmetry
$4Cu_2O/C_8$	C_s / C_1
($4Cu_2O/C_8$)-Zn	C_1
($4Cu_2O/C_8$)-ZnS	C_1
$6Cu_2O/C_{17}$	C_1
($6Cu_2O/C_{17}$)-Zn	C_1
($6Cu_2O/C_{17}$)-ZnS	C_1

Table (3) disclosures that the interaction between (Zn , ZnS) and the organic complex nanomaterial structure $4Cu_2O/C_8$ led to disappear of the point group symmetry C_s, in which the complex organic nanomaterial structures after the interaction, i.e. ($4Cu_2O/C_8$)-Zn, ($4Cu_2O/C_8$)-ZnS became own only the point group symmetry C_1. The nanomaterial structures that own the point group symmetry C_1, belong to the symmetry C_n, and the element of symmetry here is the proper axis. The point group symmetry C_1 of the nanomaterial structures showed that the symmetry occurs during (2π). The nanocluster repeat itself after (2π). The rule here, the rotation takes place during $(2\pi/n)$, therefore, in this case (n=1). In addition to C_1, one can visualize the organic complex nanomaterial structure $4Cu_2O/C_8$ has the point group symmetry C_s, in this kind of symmetry the symmetry procedure leave the nanomaterial structure the same, and the symmetry element here is the identity. This point group symmetry (C_s) is regarded important to the symmetry theoretically, although it let the nanomaterial structure the same. The importance, it expresses crucial processes, such as the double reflection of the organic complex nanomaterial structure, the symmetry plane in this point group symmetry is the mirror plane. The symmetry C_s of the organic complex nanomaterial structure ($4Cu_2O/C_8$) make it has a significance in the optics applications, and contributes to know the optical activity of substances.

H. Density of States (Dos)

Depending on the solid state physics, density of states (DOS) typifies the number of states for each energetic interval at each energy level when electrons can occupy the energy levels partially or fully [33]. In some systems, the crystal structure permits to the waves propagating in certain directions, while, the crystal structure prohibits the waves from propagating in other directions. Therefore, there is many states were founded, and the electrons might occupy these states, but there is no states in the case of prohibition the wave from propagating. The density of states possesses a maximum advantage to determine crucial physics properties, particularly in the solid state physics, just like, the HOMO energy, the LUMO energy and the energy gap [34]. Density functional theory at the ground state, B3LYP level, and 6-31G basis set, had been carried out with Gauss Sum 03 package to get the schematics o density of states (DOS) for the nanomaterial structures $4Cu_2O/C_8$, $6Cu_2O/C_{17}$, ($4Cu_2O/C_8$)-Zn, ($4Cu_2O/C_8$)-ZnS, ($6Cu_2O/C_{17}$)-Zn and ($6Cu_2O/C_{17}$)-ZnS.

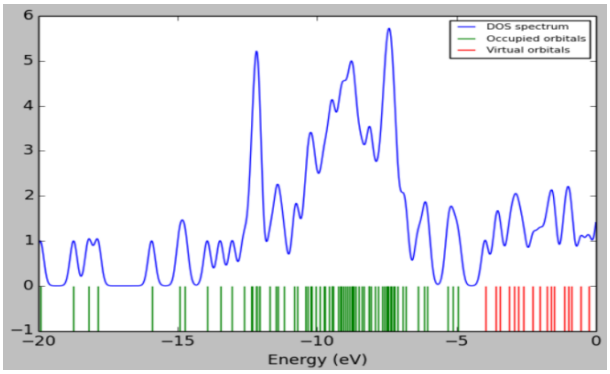

a) $4Cu_2O/C_8$

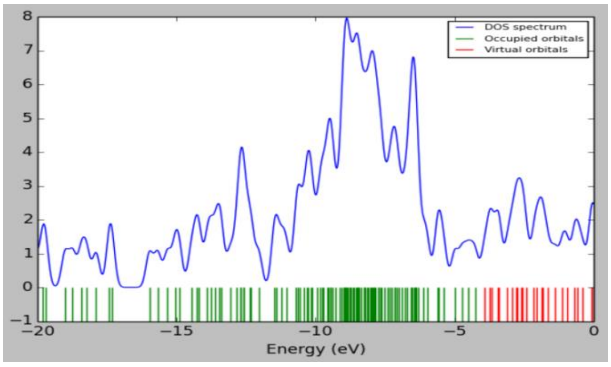

b) 6Cu2O/C17

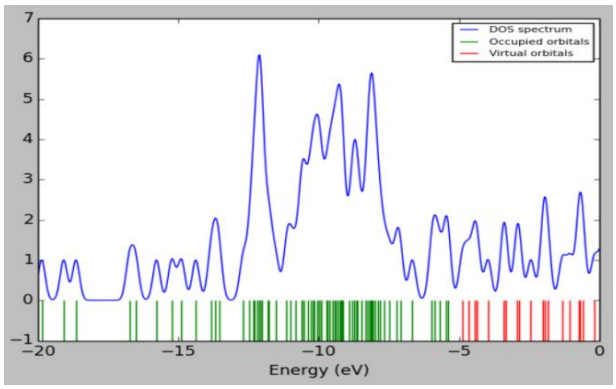

c) (4Cu2O/C8)-Zn

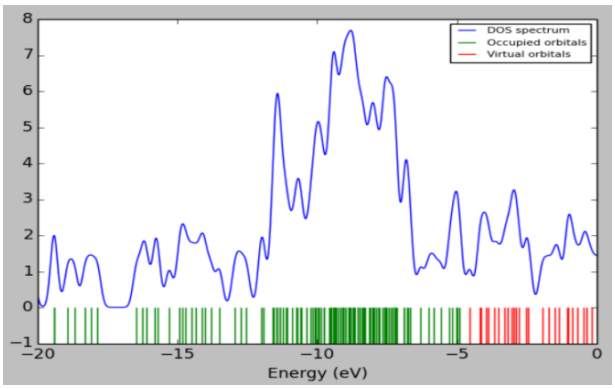

d) (6Cu2O/C17)-Zn

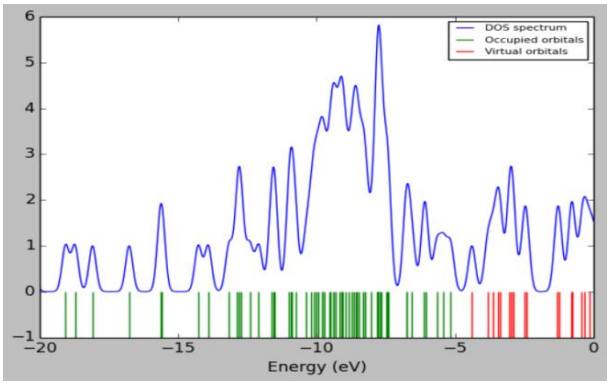

e)(4Cu2O/C8)-ZnS

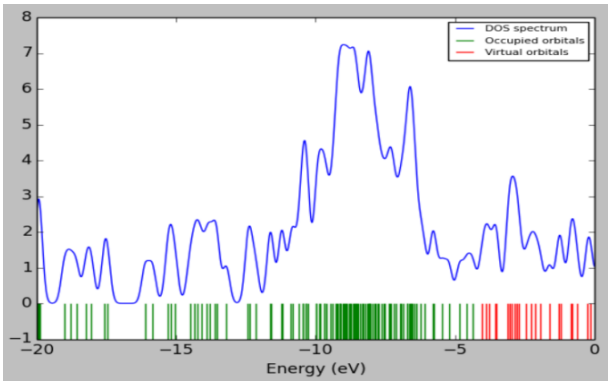

f) (6Cu2O/C17)-ZnS

Figure (5): Density of states (DOS) for the nanomaterial structures $4Cu_2O/C_8$, $6Cu_2O/C_{17}$, $(4Cu_2O/C_8)$-Zn, $(4Cu_2O/C_8)$-ZnS, $(6Cu_2O/C_{17})$-Zn and $(6Cu_2O/C_{17})$-ZnS.

Figure (5) disclosure that addition of zinc atom as impurity to the nanomaterial structures ($4Cu_2O/C_8$, $6Cu_2O/C_{17}$) causes dissimilarity in the schematics of the density of states. One can visualize new apexes demonstrate in the organic complex nanomaterial structure $(4Cu_2O/C_8)$-Zn and $(6Cu_2O/C_{17})$-Zn. These apexes are an indication of new energetic levels occupied by the electrons. One can say the electron pair in the outer shell of zinc atom in 4s orbital may transfer to fully vacant orbital in the nanomaterial structures $4Cu_2O/C_8$ or the nanomaterial structure $6Cu_2O/C_{17}$. As well it may be the electrons of copper atoms transfer to vacant orbital in the secondary shell 4p or 4d of zinc atom. One can hold a comparison between $6Cu_2O/C_{17}$ and $(6Cu_2O/C_{17})$-ZnS to find out that the number of states increase to approximately eight states in $(6Cu_2O/C_{17})$-ZnS instead of seven states in$6Cu_2O/C_{17}$ under the energy shortly (-8.5 eV). Therefor, new state demonstrates as a result to the interaction between zinc sulfide and $6Cu_2O/C_{17}$. A modest comparison between $4Cu_2O/C_8$ and $(4Cu_2O/C_8)$-ZnS summarizes new states occupied by the electrons. One can visualize there were six energetic states occupied by the electrons near the energy value (-8 eV) in the nanomaterial structure $4Cu_2O/C_8$, but there was six state demonstrated in the

nanomaterial structure ($4Cu_2O/C_8$)-ZnS under the value of energy (-13 eV). These states appeared due to the interaction between zinc sulfide atoms and the organic complex nanomaterial structure $4Cu_2O/C_8$. So, a simplified counter-posing between $6Cu_2O/C_{17}$ and ($6Cu_2O/C_{17}$)-ZnS revealed new energetic states at new values of energy as a result to the interaction between zinc sulfide and $6Cu_2O/C_{17}$.

III. Conclusions

The interaction of (zinc sulfide, zinc) with the organic complex nanomaterial structures based on copper (I) oxide/carbon led to hetro-junctions that have a significant interest in the electrochemical and photocatalytic characteristics. As well the interaction between (zinc sulfide, zinc) with the organic complex nanomaterial structures based on copper (I) oxide/carbon causes dissimilarity in the electronic charge distribution around the nuclei of atoms. The electronic charge distribution demonstrated by the electrostatic potential surfaces and contour maps. The new peaks in the diagrams of infrared spectra (IR) signs new bonds originated by the interaction between (zinc sulfide , zinc) with the organic complex nanomaterial structures based on copper (I) oxide/carbon. Some of nanomaterial structures summarized the values of energy band gaps in the range of semiconductor materials, and this made them acquire an importance in the electronic devices such as, sensors, detectors and energy storage devices. The complex organic nanomaterial structures on ($6Cu_2O/C_{17}$), ($6Cu_2O/C_{17}$)-ZnS and ($6Cu_2O/C_{17}$)-Zn showed high values average polarizabilities as compared with the organic complex nanomaterial structure ($4Cu_2O/C_8$), ($4Cu_2O/C_8$)-ZnS and ($4Cu_2O/C_8$)-Zn. The highest activity nanomaterial structure among them is ($6Cu_2O/C_{17}$)-ZnSIit had average polarizability approximately (1566.18 a.u). All nanomaterial structures in this research had non-zero dipole moment because they were hetronuclear nanomaterial structures. The highest dipole moment nanomaterial structure was ($4Cu_2O/C_8$)-ZnS, and it owned the value (15.34 Debye). All nanomaterial structures had the symmetry C_1, except ($4Cu_2O/C_8$) which possessed the point group symmetry C_s in addition to C_1. This made it acquire a significant interest in the optics devices. There were many new energetic states demonstrated after the interaction between (zinc sulfide , zinc) and the organic complex nanomaterial structures based on copper (I) oxide/carbon.

Conflicts of interest

The authors declare that they have no conflict of interest.

References

[1] M. Assadi, "Theoretical study on copper's energetic and magnetism in TiO2 polymorphs," *J. Appl. Phys. , vol. 113, no. 23, p. 233913,* 2013.

[2] Q. Xu, C. Ma, W. Mi, Y. Wang, and Y. Ma, "Recent advancements and challenges in orbital-free density functional theory," *Wiley Interdiscip. Rev. Comput. Mol. Sci., vol. 14, no. 3, p. e1724,* 2024.

[3] M. Skogh, W. Dobrautz, P. Lolur, C. Warren, J. Biznárová, A. Osman, et al., "The electron density: a fidelity witness for quantum computation," *Chem. Sci., vol. 15, no. 6, pp. 2257–2265,* 2024.

[4] V. Butera, "Density functional theory methods applied to homogeneous and heterogeneous catalysis: a short review and a practical user guide," *Phys. Chem. Chem. Phys., vol. 26, no. 10, pp. 7950–7970,* 2024.

[5] M. Holthausen and W. Koch, *A Chemist's Guide to Density Functional Theory*, Weinheim, Germany: Wiley–VCH, 2001.

[6] M. Ali, "Investigations of some antioxidant materials by using density functional and semiempirical theories," *Ph.D. dissertation, Dept. Phys., Univ. Basrah, Basrah,* Iraq, 2009.

[7] K. Lejaeghere, G. Bihlmayer, T. Björkman, P. Blaha, S. Blügel, V. Blum, et al., "Reproducibility in density functional theory calculations of solids," *Science, vol. 351, no. 6280, p. aad3000,* 2016.

[8] G. Stefan, "Semiempirical hybrid density functional with perturbative second order correlation," *J. Chem. Phys., vol. 124, no. 3, p. 034108*, 2006.

[9] I. J. Casely, J. W. Ziller, M. Fang, F. Furche, and W. J. Evans, "Synthesis of organometallic complexes," *J. Am. Chem. Soc., vol. 133, p. 5244,* 2011.

[10] C. J. Cramer, Essentials of Computational Chemistry, Chichester, U.K.: John Wiley & Sons, 2002.

[11] A. S. Alwan, "Density functional theory investigation of (C4H2N2)3 nanocluster and (C4H2N2)3—P, Al, As, B, C and in nanoclusters," *in AIP Conf. Proc., vol. 2292, no. 1, Oct.* 2020.

[12] Y. B. Hahn, "Zinc oxide nanostructures and their applications," *Korean J. Chem. Eng., vol. 28, no. 9, p. 1797,* 2011.

[13] G. Naresh, P. L. Hsieh, V. Meena, S. K. Lee, Y. H. Chiu, M. Madasu, et al., "Facet-dependent photocatalytic behaviors of ZnS-decorated Cu2O polyhedra arising from tunable interfacial band alignment," *ACS Appl. Mater. Interfaces, vol. 11, no. 3, pp. 3582–3589,* 2018.

[14] R. Bengas, H. Lahmar, K. M. Redha, L. Mentar, A. Azizi, G. Schmerber, and A. Dinia, "Electrochemical synthesis of n-type ZnS layers on p-Cu2O/n-ZnO heterojunctions with different deposition temperatures," *RSC Adv., vol. 9, no. 50, pp. 29056–29069*, 2019.

[15] Y. Zhu, L. Wang, W. Xu, Z. Xu, J. Yuan, and G. Zhang, "ZnO/Cu2O/g-C3N4 heterojunctions with enhanced photocatalytic activity for removal of hazardous antibiotics," *Heliyon, vol. 8, no. 12,* 2022.

[16] G. Du, P. Gong, C. Cui, L. Wang, and C. An, "Solid-state construction of CuO–Cu2O@C with synergistic effects of pseudocapacity and carbon

coating for enhanced electrochemical lithium storage," *Nanomaterials, vol. 14, no. 17, p. 1378*, 2024.

[17] M. J. Frisch et al., *Gaussian 09, Revision D.01, Wallingford, CT, USA: Gaussian, Inc.*, 2009.

[18] T. Scheele and T. Neudecker, "Investigating the accuracy of density functional methods for molecules in electric fields*," J. Chem. Phys., vol. 159, no. 12*, 2023.

[19] M. Nakata and T. Maeda, "PubChemQC B3LYP/6-31G//PM6 data set: The electronic structures of 86 million molecules using B3LYP/6-31G calculations," *J. Chem. Inf. Model. vol. 63, no. 18, pp. 5734–5754*, 2023.

[20] A. Szabo and N. S. Ostlund, *Modern Quantum Chemistry: Introduction to Advanced Electronic Structure Theory, Mineola, NY, USA*: Dover, 2012.

[21] A. B. Ahmed, "Studying the electronic characteristics and physisorption of OTS on the pure silver surfaces (Ag10), (Ag15), and (Ag18*)," Univ. Thi-Qar J. Sci., vol. 10, no. 2, pp. 151–159*, 2023.

[22] A. G. Borisov, A. K. Kazansky, and J. P. Gauyacq, "Resonant charge transfer in ion-metal surface collisions: Effect of a projected band gap in the H−Cu(III) system," *Phys. Rev. B, vol. 59, pp. 10935–10942*, 1999.

[23] A. S. Alwan, "Density functional theory investigation of (C4H2N2)3 nanocluster and (C4H2N2)3—P, Al, As, B, C and in nanoclusters," *in AIP Conf. Proc., AIP Publishing LLC, p. 30013*, 2020.

[24] K. Mohsin and H. I. Aboud, "Density functional study on molecular interactions," *Int. J. Pure Appl. Sci. Technol., vol. 15, no. 1, pp. 1–13,* 2013.

[25] M. L. Jabbar, "Some electronical properties for Coronene-Y interactions by using density functional theory (DFT)," *J. Basrah Res., vol. 44, no. 1*, 2018.

[26] S. M. Sze, Semiconductor Devices: *Physics and Technology, 2nd ed., Hoboken, NJ, USA: John Wiley & Sons*, 2008.

[27] H. M. Jawad, T. A. Husain, and I. N. Qader, "Study of physical and electrical properties of sandwich compound as drug delivery to transport chlorpheniramine medication using density functional theory," *J. Phys. Chem. Funct. Mater., vol. 6, no. 2, pp. 124–131*, 2023.

[28] S. Grimme, "Semiempirical hybrid density functional with perturbative second order correlation*," J. Chem. Phys., vol. 124, no. 3, p. 034108*, 2006.

[29] S. Gümüş, "A computational study on substituted diazabenzenes," *Turk. J. Chem., vol. 35, no. 5, pp. 803–808*, 2011.

[30] Review Notes on Point Groups and Symmetry from undergraduate Inorganic Chemistry I course, *The Ohio State Univ., unpublished notes*.

[31] A. Pausch, M. Gebele, and W. Klopper, "Molecular point groups and symmetry in external magnetic fields," *J. Chem. Phys., vol. 155, no. 20*, 2021.

[32] A. M. Lesk, Introduction to Symmetry and Group Theory for Chemists, New York, NY, USA: Springer, 2004.

[33] B. Ahmed, "Studying the electronic characteristics and physisorption of OTS on the pure silver surfaces (Ag10), (Ag15), and (Ag18)," *Univ. Thi-Qar J. Sci., vol. 10, no. 2, pp. 151–159*, 2023.

[34] M. Y. Toriyama, A. M. Ganose, M. Dylla, S. Anand, J. Park, M. K. Brod, et al., "How to analyse a density of states," *Mater. Today Electron., vol. 1, p. 100002*, 2022.